



Synthesis, characterization and adsorption studies of nano-composite hydrogels and the effect of SiO₂ on the capacity for the removal of Methylene Blue dye

SINAN TEMEL¹, ELIF YAMAN¹, NURGUL OZBAY² and FATMA OZGE GOKMEN^{1*}

¹Central Research Laboratory, Bilecik Seyh Edebali University, 11230, Bilecik, Turkey and

²Chemical Engineering Department, Bilecik Seyh Edebali University, 11230, Bilecik, Turkey

(Received 17 May; revised 12 October; accepted 24 October 2019)

Abstract: Nanocomposite hydrogels were produced by free radical polymerization of acrylic acid and *N*-vinylpyrrolidone in the presence of SiO₂ nanoparticles. The chemical and morphological structures of the hydrogels were determined using Fourier transform infra-red spectroscopy (FT-IR) and field emission scanning electron microscopy (FESEM). The nanocomposite hydrogels were used for the adsorption and desorption of Methylene Blue dye from wastewater. Wastewater was referred to distilled water that contained Methylene Blue dye under laboratory conditions. The carbon, hydrogen and nitrogen contents of the dye, hydrogels and dye-adsorbed hydrogels were determined by elemental analysis. The influences of SiO₂ nanoparticles and copolymerization on the adsorption capacity were studied. The maximum dye removal of 98.3 % was obtained with AA-co-VP (3:1) copolymeric hydrogel. The synthesized hydrogels could be evaluated as adsorbents in wastewater treatment, effectively.

Keywords: wastewater treatment; textile dyes; acrylic acid hydrogels; vinyl pyrrolidone; SiO₂ nanoparticles.

INTRODUCTION

Textile dyes are very toxic to aquatic life in waters and carcinogenic for human health.¹ Dye molecules disperse into water and cause pollution in surface, ground, and drinking water. More than 100,000 types of dyes are utilized in different industries, such as paper, leather, pharmaceutical, cosmetic, and textile.^{2–5} A great number of coloured components generated by textile industries are directly delivered to water.⁶ In addition, the degradation of some organic dyes indicates to a potential environmental hazard due to the products containing aromatic amine compounds.⁷ Despite a number of dyes that are prohibited in most countries due to health hazards, others where the use of the dyes are not prohibited generate hazardous components that are hardly treated using conventional

* Corresponding author. E-mail: fatmaozge.gokmen@bilecik.edu.tr
<https://doi.org/10.2298/JSC190517114T>

biological treatments through their stability to light, heat, and oxidizing agents.^{7,8} Among the various dyes, one of the most used thiazine cationic dye is Methylene Blue (MB) in the textile industry. MB dye causes some health problems, such as eye burns, respiratory insufficiency, nausea, vomiting, and mental confusion even after exposure to small amounts.^{9,10} Various methods can be used for the removal of dyes from water, such as coagulation, precipitation, electrode-deposition, membrane filtration,¹¹ ion exchange,¹² solvent extraction,¹³ electro-dialysis,¹⁴ advanced oxidation processes,⁵ *etc.* In recent years, adsorption is one of the most simple, easy and economical methods. This method has advantages such as providing regeneration, being sludge free and high efficiency when applied with a proper adsorbent.^{8,15} Adsorbents produced from synthetic and natural biopolymers can be used for the adsorption of dyes from waste water.¹⁶ Adsorbents should be recovered after the adsorption process. An attractive proposal uses hydrogel materials as adsorbents in wastewater treatment due to reproducibility.¹⁷ Stimuli-responsive hydrogels, also called “intelligent hydrogels”, are highly important materials in various application areas, such as medicine, biotechnology, sensor, agriculture and adsorbent industry.¹⁸ Recently, nanocomposite hydrogels have been largely utilized in several applications.^{19–23} These hydrogels are 3-D networks of hydrophilic polymers that can absorb and preserve a huge amount of water in the presence of nanoparticles (NPs). The doping of NPs into the hydrogel supplies great mechanical strength and higher adsorption capacity.²⁴ Various methods have been studied for the preparation of hydrogels. One of them comprises copolymerization/crosslinking of monomers using multi-functional co-monomers, which is used with a crosslinking agent. In this approach, polymerization is initiated chemically. The polymerization reaction can be executed in bulk, solution, or suspension. The other approach comprises the crosslinking of linear polymers by irradiation or by chemical components.^{25–29}

In this work, nano-SiO₂ doped AA and AA-*co*-VP nanocomposite hydrogels were synthesized with the purpose of the adsorption of MB dye from wastewater. AA was chosen as a highly hydrophilic co-monomer that supports high swelling, VP as a polar hydrophilic co-monomer that could provide polar interactions with dyes, while the SiO₂ nanofiller should enhance the adsorption of dyes and other polar compounds. The effect of copolymerization and doping ratio of nano SiO₂ in hydrogels were optimized to obtain the highest adsorption capacity of the nanocomposite hydrogels.

EXPERIMENTAL

The hydrogel samples were synthesized by crosslinking copolymerization of *N*-vinylpyrrolidone with *N,N*-methylene-bis-acrylamide (MBA) in aqueous solution using ammonium persulphate (APS) as a radical initiator.

Materials

Acrylic acid (AA), *N*-vinylpyrrolidone (VP), ammonium persulphate (APS), *N,N*-methylene-bis-acrylamide (MBA), SiO₂ nanoparticles (20–30 nm) were purchased from Aldrich, Methylene Blue (MB) dye was purchased from Sigma–Aldrich.

Preparation of hydrogels and SiO₂-doped nanocomposite hydrogels

The AA and AA-*co*-VP hydrogels were synthesized by free radical polymerization in the presence of an initiator and crosslinking agent in aqueous solution. All chemicals according to Table I were mixed at the same time by brief stirring and filled in PVC straws. The PVC straws were placed in a water bath that was set at 80 °C. The ratio of AA-*co*-VP was optimized to values of 3:1, 2:2 and 1:3. The concentration of polymerisable double bonds (including the crosslinker) was always kept constant at 5.56 M. The initiator concentration was always 0.01M. The reaction mixtures were held at 80 °C for 4 h. After completion of the reaction, the PVC straws were cooled down to room temperature and hydrogels were released from the straws. The obtained hydrogels were cut in the same diameter (3–4 mm) and dried under ambient conditions for 24 h.

TABLE I. Formulations for the synthesis of the hydrogel; 0.0308 g MBA (cross-linking agent); 0.0091 g APS (initiator); water filled-up to a total volume of the reaction mixture of 4 mL

Hydrogel ID	Amount of AA, g	C _{AA} mmol	Amount of VP, g	C _{VP} mmol	Amount of SiO ₂ nanoparticle, g
AA	1.59	22	–	–	–
AA-SiO ₂ (0.05)	1.59	22	–	–	0.002
AA-SiO ₂ (0.5)	1.59	22	–	–	0.021
AA-SiO ₂ (1)	1.59	22	–	–	0.041
AA-VP _(3:1)	1.19	16.5	0.61	5.5	–
AA-VP _(2:2)	0.79	11	1.22	11	–
AA-VP _(1:3)	0.40	5.5	1.83	16.5	–
AA-VP-SiO ₂ (0.05)	1.19	16.5	0.61	5.5	0.002
AA-VP-SiO ₂ (0.5)	1.19	16.5	0.61	5.5	0.021
AA-VP-SiO ₂ (1)	1.19	16.5	0.61	5.5	0.041

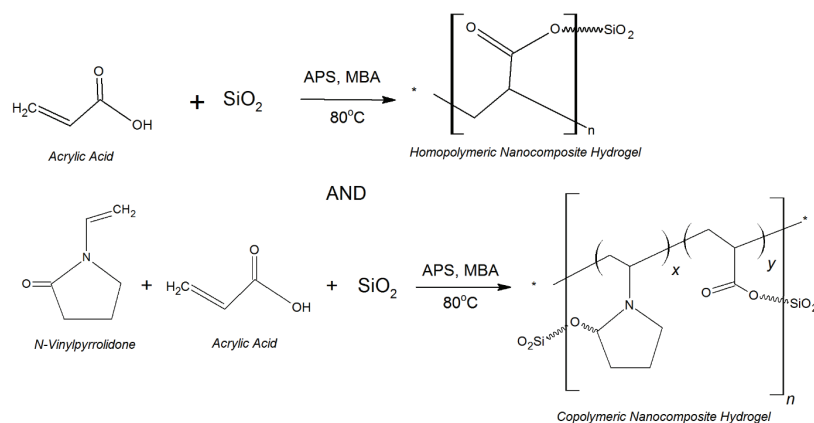
The SiO₂-doped nanocomposite hydrogels were synthesized in the same way as the SiO₂-free ones. The only synthesis difference was the addition of nano-SiO₂ (see Table I for the amounts). The dispersion of SiO₂ in the solution was achieved during an initial brief stirring of the components of the reaction mixture. The experimental details were given in a previous study.²⁵ Schematic representations of the possible structures of the homo- and copolymeric hydrogels is given in Scheme 1.

Characterization

Fourier transform infrared spectroscopy (FT-IR) measurements were performed in a Perkin Elmer Spectrum 100 FT-IR spectrometer over the range from 400–4000 cm⁻¹ with the attenuated total reflectance (ATR) module under the conditions of 4 scans with a spectral resolution of 4 cm⁻¹.

The morphology of hydrogel surface and elemental analysis were investigated using a field emission scanning electron microscopy (Zeiss, Supra 40VP) under a 15-kV electron acceleration voltage after Au/Pd (80/20) coating of the sample. Prior to observation, the swollen hydrogels were put in a freezer (kept at –18 °C) for 12 h, then placed in a vacuum device

in the frozen state (instrument: Labconco, Freezone 2.5 (Canada) lyophilizer). After 16 h of freeze-drying, the hydrogels were examined by FESEM.



Scheme 1. Schematic illustration of the preparation of crosslinked homo/co-polymeric hydrogels.

The carbon, hydrogen and nitrogen contents of dye, hydrogels and dye-adsorbed hydrogels were determined by elemental Analysis (LECO, CHNS 628).

Swelling behaviour

The swelling behaviour of the hydrogels in water was followed for 56 h at room temperature. The swelling ratio (S , %) was calculated using Eq. (1):

$$S = 100 \frac{m_t - m_1}{m_1} \quad (1)$$

where m_t is the mass of the swollen hydrogels at time t and m_1 is the initial mass of the hydrogels.

Methylene Blue (MB) adsorption

The batch adsorption studies of MB were carried out by placing nanocomposite hydrogels (AA, AA-SiO₂, AA-co-VP, AA-co-VP-SiO₂) in an aqueous solution of MB. The initial concentrations of MB were 2–10 mg L⁻¹ tested for adsorption by ≈70 mg of hydrogels. The dry hydrogels were submerged into 10 mL of MB solution and allowed to equilibrate for 56 h at room temperature. The pH of the solution was 8.4. The equilibrium time was specified as 25 h for each hydrogel. The concentration of Methylene Blue in the supernatant was determined on a UV–Vis spectrometer (Perkin Elmer, Lambda 25) at a detection wavelength of 664 nm. The quantity of Methylene Blue dye adsorbed was determined using Eq. (2):

$$q_t = \frac{C_0 - C_t}{m} V \quad (2)$$

where q_t is the adsorption quantity at time t / mg g⁻¹, C_0 is the initial concentration of Methylene Blue dye solution, mg L⁻¹; C_t / mg L⁻¹ is the Methylene Blue concentration at time t , V / L is the volume of the Methylene Blue solution, and m / mg is the mass of adsorbent.

The equilibrium adsorption amount of Methylene Blue dye for the determination of the isotherms was calculated using Eq. (3):

$$q_e = \frac{C_0 - C_e}{m} V \quad (3)$$

where q_e is the equilibrium adsorption amount, mg g^{-1} , and C_0 and C_e are the initial and equilibrium concentrations of the MB dye solution (mg L^{-1}). All sorption experiments were conducted in duplicate.

Desorption and reusability of Methylene Blue loaded hydrogels

Desorption studies of SiO_2 doped and undoped AA homopolymeric nanocomposite hydrogels containing 2, 4, 6, 8 and 10 mg L^{-1} dye were performed. The effect of SiO_2 addition on desorption was investigated. To specify the reusability of the hydrogels, 8 sequential cycles were performed. In each cycle, Methylene Blue dyed loaded hydrogels were taken into 10 mL aqueous solution (pH 6.4) and 24 h was waited for equilibration of the desorption. At the end of the equilibration time, the sorbent was separated from dye and the residual Methylene Blue dye concentration in the supernatant was measured. The percentage of dye adsorption was determined by measuring the absorption of the solution 664 nm using a UV-Vis spectrophotometer (Perkin Elmer, Lambda 25) and calculated using Eq. (4):

$$\text{Removal, \%} = 100 \frac{C_0 - C_e}{C_0} \quad (4)$$

RESULTS AND DISCUSSION

In this study, SiO_2 -doped acrylic acid and acrylic acid-*co*-vinyl pyrrolidone (AA-*co*-VP) nanocomposite hydrogels were synthesized by the free radical polymerization technique. Experimental conditions were optimized as a temperature of 80 °C and a reaction time of 4 h without stirring. Chemical components of polymerization were 5.5 M monomer, 0.05 M crosslinking agent and 0.01 M initiator.

Swelling behaviour

Swelling tests of hydrogels and nanocomposite hydrogels were performed at room temperature with deionised water. The swelling behaviours of the gels were monitored for 56 h. The equilibrium of the swollen was achieved after 25 h. The swelling values of the hydrogels in water were calculated according to Eq. (1). According to Fig. 1, as expected, hydrogel (AA hydrogel) and co-polymeric hydrogel (AA-*co*-VP (3: 1) hydrogel) had the highest swelling value.

Unexpected results for AA-*co*-VP-1% SiO_2 showed that 1 % of the nanoparticles were non-homogeneously agglomerated in the hydrogel pores. SiO_2 nanoparticles dispersed in the pores of hydrogels increased the surface area and reduced the pore diameter. In such cases, the doped hydrogels exhibited lower swelling behaviour than the undoped hydrogels.

FT-IR and FESEM analyses

The FT-IR spectrum of the Methylene Blue dye (black line) and that of the non-adsorbed AA-*co*-VP (3: 1) hydrogel (red line) are shown in Fig. 2a. The spectrum of Methylene Blue adsorbed on AA-*co*-VP (3: 1) hydrogel is shown in

Fig. 2b. The FT-IR spectra of the other hydrogels and nanocomposite hydrogels synthesized in this study are given in the Supplementary material to this paper, Fig. S-1. The wide bands at 3059, 2923 and 2846 cm^{-1} comply with the CH_3 stretching vibrations of dimethylamino groups of MB. The peaks at 2812 and 2701 cm^{-1} accord with the heterocyclic $\text{C-N}-(\text{CH}_3)_2$ vibrations. The region of 1440–1650 cm^{-1} contains free molecules of MB dye.³⁰ The intense band with a peak at 1584 cm^{-1} accords with the C=N and C=C vibrations of the MB heterocycle. The band at 1490 cm^{-1} accords with the C-N vibrations MB. The peaks at 1337 and 1379 cm^{-1} accord with the C-N and C=S^+ stretching vibrations of MB. In addition, C-N and C-S-C vibrations of the MB^+ heterocycle are visible at 876 and 1132 cm^{-1} , respectively.

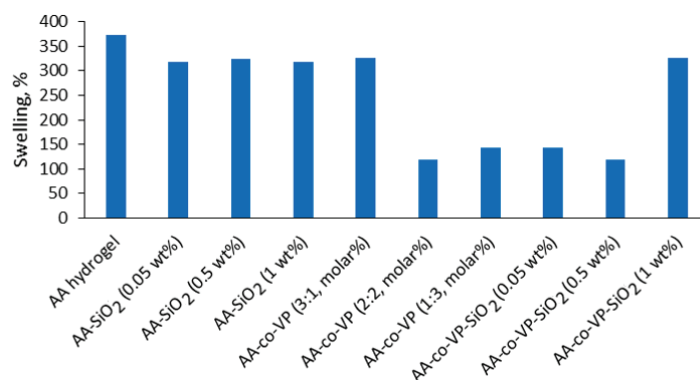


Fig. 1. Swelling behaviour of AA and AA-co-VP nanocomposite hydrogels; maximal swelling degree of hydrogels at equilibrium time (25th h).

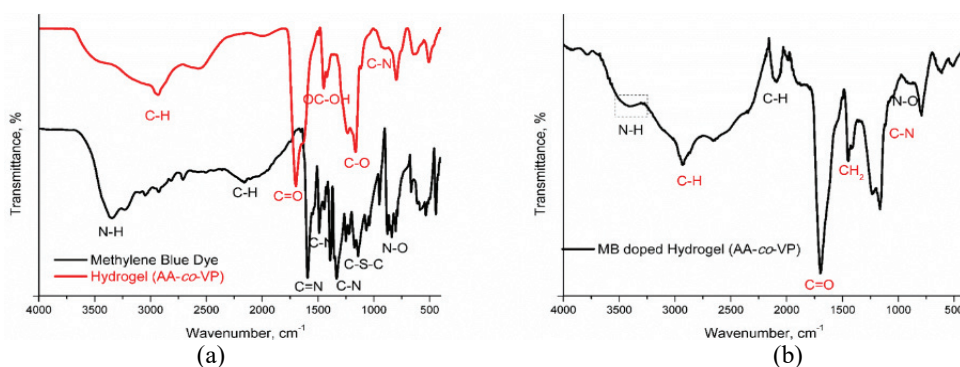


Fig. 2. a) FT-IR spectra of MB dye and hydrogel (AA-co-VP (3:1)) and b) MB adsorbed AA-co-VP (3:1) hydrogel.

The strong absorption band visible in the range 1475–1780 cm^{-1} is due to the -C=O of VP and carboxylic acid of AA. The peak at 1439 cm^{-1} demonstrates the OC-O-H stretching vibration. The peak at 3440 cm^{-1} is due to the -OH band

of AA. The peak at 1481 cm^{-1} belongs to the tertiary amine groups of VP. The peak at 1149 cm^{-1} with a shoulder accords with the stretching vibration of the C–O of PAA.

SEM image of Methylene Blue at $1000\times$ magnification is given in Fig. 3. The EDX spectrum of the dye shows that the average values of the chemical content of the dye. According to these values, the increase of the N content in the dye-adsorbed hydrogels proves the presence of the dye on the hydrogel, as given in Table II.

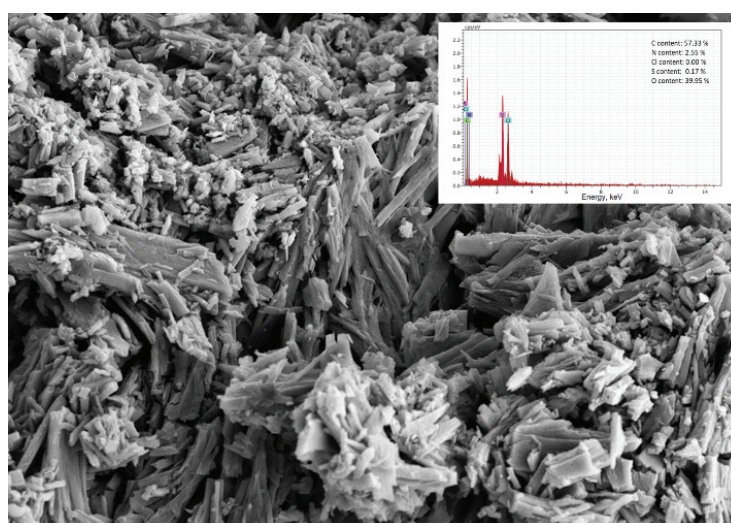


Fig. 3. SEM image and EDX spectrum of MB.

TABLE II. Elemental contents except hydrogen before and after MB adsorption on AA mono polymeric hydrogels

Element	Content, wt. %	
	Before	After
C	59.12	57.65
N	0.00	2.47
O	40.88	39.87

The morphological structure of the MB dye not adsorbed/adsorbed on AA monopolymeric hydrogels can be seen in Fig. 4a and b. The AA monopolymeric hydrogel was chosen for SEM analysis, because of the absence nitrogen in their chemical structure. Therefore, differences between doped/undoped hydrogels were determined by EDX analysis.

The hydrogels with absorbed MB lost their elasticity. In addition, the porous structure generated by freeze-drying of the gels loaded with MB was different and less homogeneous than the porous structure generated by freeze-drying of

MB-free gels (compare Fig. 4a and b). The different porosity of the dried MB-loaded gels well correlates with their observed stiffness in the swollen state.

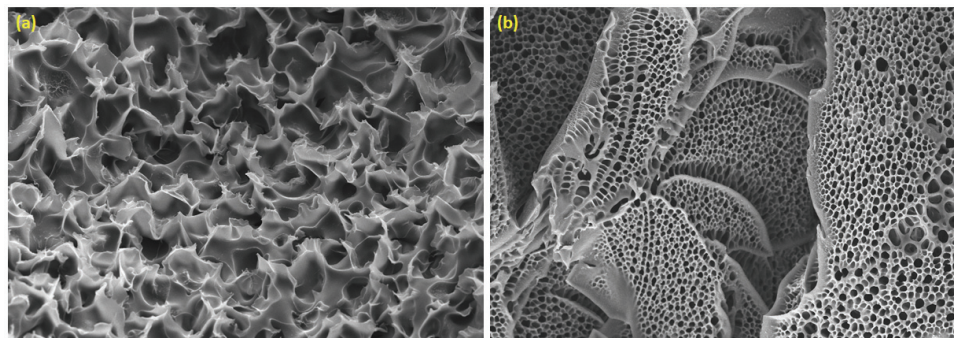


Fig. 4. SEM images of lyophilized: a) AA hydrogel before MB adsorption and b) AA hydrogel after MB adsorption.

The images in Fig. S-4 of the Supplementary material taken at 5000 magnification belong to copolymeric hydrogels prepared in three different ratios (AA-*co*-VP (3:1), (2:2) and (1:3)). Among the copolymeric hydrogels, AA-*co*-VP (3:1) had the highest number of pores in its structure. The swelling behaviour of AA-VP, which has the highest percent swelling value among copolymeric hydrogels, was also proved morphologically. Unexpectedly, the percent swelling value of the copolymeric nanocomposite hydrogel containing 1 % SiO₂ was the same as for the pure hydrogel. This is because SiO₂ cannot be homogeneously distributed in the hydrogel structure.

The chemical contents before and after the dye adsorption process are given in Table II. Accordingly, the increments of the nitrogen content (2.47 %) evidenced the adsorption of Methylene Blue dye onto the hydrogels.

Adsorption studies

The adsorption studies were performed using 2, 4, 6, 8 and 10 mg L⁻¹ aqueous solutions of MB under ambient conditions. Batch adsorption studies were performed to optimize the experimental parameters, such as the doping ratio of SiO₂. The used adsorbent dose was similar in all batch experiments (≈ 70 mg). In all batch experiments, the swollen hydrogel was submerged in 10 mL of dye solution.

Removal values of MB dye on hydrogels are given in Table III. As could be seen in Table III, the maximum dye removal was obtained with undoped hydrogels, due to their superior swelling properties. In comparison, the maximum dye removal was obtained with AA-*co*-VP (3:1), which includes more anionic groups than the other copolymers. It is possible to explain dye interaction between anionic adsorbent and cationic dye. The SiO₂ addition (1, 0.5 and 0.05 wt. %) in the

TABLE III. Removal values (%) of MB dye by the hydrogels

C mg L ⁻¹	Hydrogel												
	AA 0.05 % SiO ₂	AA 0.05 % SiO ₂	AA 0.5 % SiO ₂	AA 1 % SiO ₂	AA 1 % SiO ₂	AA-co-VP (1:3)	AA-co-VP (2:2)	AA-co-VP (3:1)	AA-co-VP (3:1)	AA-co-VP (3:1)	AA-co-VP (3:1)	AA-co-VP (3:1)	AA-co-VP (3:1)
2	77.8	77.8	80.5	75.5	82.0	82.0	76.0	82.5	87.5	88.5	87.5	88.5	87.5
4	77.5	77.2	81.0	67.7	87.7	87.7	91.0	92.2	90.7	91.0	90.7	91.0	94.2
6	81.5	84.0	83.6	76.8	92.7	92.7	93.5	92.2	88.7	95.2	88.7	95.2	94.0
8	78.1	75.0	82.5	75.4	96.7	96.7	93.7	91.7	84.1	95.0	84.1	95.0	86.4
10	80.8	79.4	77.6	77.5	98.3	98.3	92.8	94.3	89.6	96.7	89.6	96.7	89.8

hydrogels was kept to low amounts due to agglomeration. Therefore, the adsorption amount of hydrogels did not change greatly on varying the MB dye concentrations (2, 4, 6, 8 and 10 mg L⁻¹).

Adsorption isotherms

The adsorption isothermal studies were performed without shaking in a series of vials by adding the chosen quantity of adsorbent (≈ 70 mg) and 10 mL of MB solution of different concentrations (2, 4, 6, 8 and 10 mg L⁻¹) at 25 °C and pH 8.4 until equilibrium was attained. The UV–Vis absorbance of the samples was measured over three days and the concentrations of MB were determined. The equilibration time was 25 h for each hydrogel. The adsorption capacity of adsorbent for MB was determined using Eq. (3). The isotherms of SiO₂ doped and undoped hydrogels in MB dye solution are shown in Fig. 5.

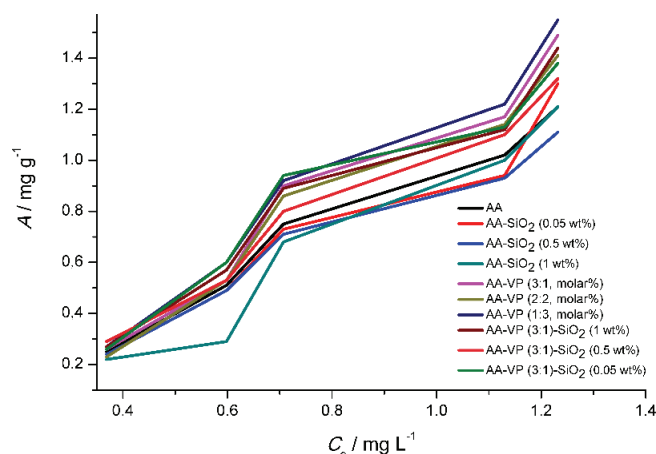


Fig. 5. Isotherms of SiO₂-doped and undoped hydrogels in MB dye solution.

Reusability of hydrogels

The MB desorption studies were performed with hydrogels previously equilibrated in 2, 4, 6, 8 and 10 mg L⁻¹ MB dye solutions at pH 8.4. The desorption was performed in distilled water (pH 6.4) in eight cycles of 24 h per cycle. The amount of desorbed MB dye was determined by UV–Vis spectrometry. The recovery range was between 25–40 % for various dye loadings (Fig. 6).

At lower concentrations, the dye recovery was in the range of 35–40 % (Fig. 6). The maximum recovery values were obtained from undoped (SiO₂-free) hydrogels. As the amount of SiO₂ increased, the recovery was reduced by about 5 % (Fig. 6). The SiO₂ nanoparticles obviously bonded the Methylene Blue more strongly than the (AA, AA-co-VP) polymer chains. While at pH 8.4, the adsorption was highly efficient (80–98 % observed), in case of distilled water at pH 6.8,

the reverse process (desorption) was moderately favoured: maximum released MB amounts of 40 % were achieved. This demonstrates the pH-sensitivity of the adsorption process.

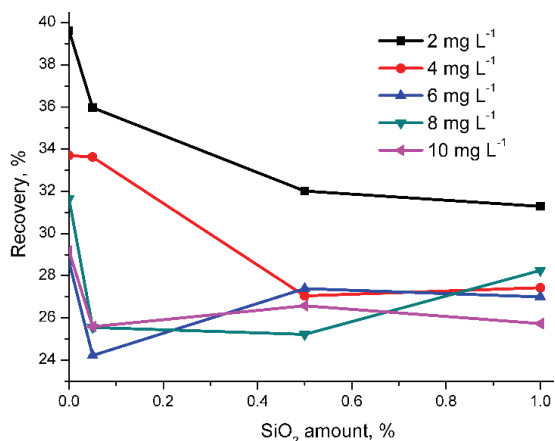


Fig. 6. Effect of SiO₂-doping ratio on dye desorption on SiO₂-doped AA homo-polymeric hydrogels.

Elemental analysis (C, H, N)

The C, H and N weight contents of the dye-adsorbed hydrogels were determined by elemental analysis. The amount of nitrogen arising from MB was determined in both homo and co-polymeric doped and undoped SiO₂ hydrogels.

The elemental N distributions of the dye-adsorbed hydrogels are given in Fig. 7. As could be seen, the amount of nitrogen showed the presence of the dye on all hydrogels but in different amounts, whereby the amount of dye attached to AA-co-VP/SiO₂ (1 wt. %) co-polymeric hydrogel was the greatest.

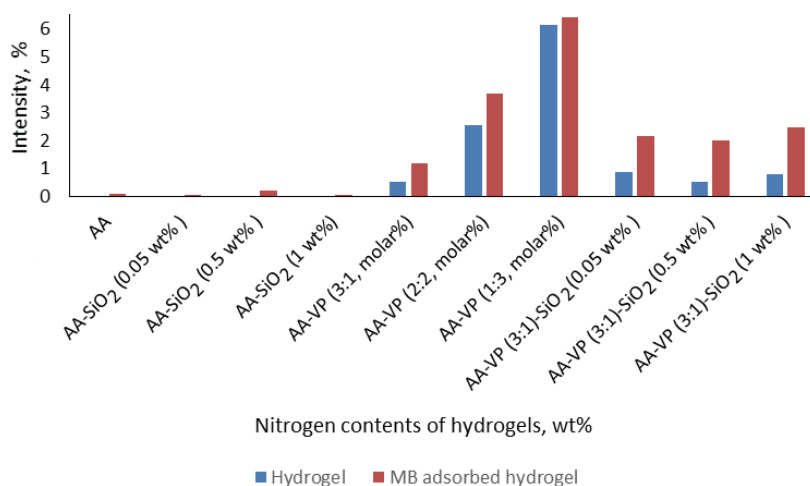


Fig. 7. Nitrogen contents in non-adsorbed hydrogel and MB adsorbed hydrogel.

CONCLUSIONS

SiO₂-doped acrylic acid and acrylic acid-*co*-vinyl pyrrolidone nanocomposite hydrogels were synthesized by the free radical polymerization technique. The experimental conditions were optimized as a temperature of 80 °C and a reaction time of 4 h without stirring. FT-IR spectroscopy and SEM analysis proved the successful synthesis of nanocomposite hydrogels. Copolymers (AA-*co*-VP (3:1)) showed similar behaviour to the homopolymer but they possessed some new characteristics, which are based on the interaction between the co-monomers and the adsorbed dyes. The SiO₂-free (both homo-polymeric and co-polymeric) hydrogels showed a higher swelling than SiO₂-doped nanocomposite hydrogels, due to some physical crosslinking by the SiO₂ nanoparticles in the nanocomposite hydrogels. Of the copolymeric hydrogels, AA-*co*-VP (3:1) has the highest number of pores in its structure. The percent swelling value of the copolymeric nanocomposite hydrogel containing 1 % SiO₂ was the same as for the pure hydrogel. Adsorption of Methylene Blue on SiO₂-free and on nanocomposite hydrogels was proved by comparing the amounts of C, H, N. Due to existence of anionic functional groups, the acrylic acid-based nanocomposite hydrogels behaved as adsorbents for cationic dyes (MB) from aqueous solutions. The hydrogels showed high MB adsorption ability. The cross-linked hydrogel network was expanded in water, and the adsorption of MB was realized. Positively charged of MB dye were adsorbed by anionic carboxylic centres of the hydrogels. The best dye adsorption was obtained with the AA-*co*-VP (3:1) copolymeric hydrogel at a concentration of 10 mg L⁻¹. The copolymeric hydrogels adsorbed about 15–20 % more MB dye than the mono polymeric hydrogels. This shows that the composite formed by combining two monomers of different properties was advantageous to using single monomers. It could be stated that with increasing amount of SiO₂ in the adsorbent, the dye holding property of the adsorbent increased. In the desorption studies, interactions between SiO₂ and the MB dye were clearly stronger than those between the hydrogels and the MB dye. The SiO₂ nanoparticles showed excellent adsorbent properties. When the EDX result and the CHN result are compared, it could be seen that they are corrected to each other. Considering the FT-IR results, the presence of N peaks of the MB dye was observed on the hydrogels. Experimental results showed that the MB adsorption followed non-linear isotherm curves, revealing the adsorption occurred through monolayer and multilayer adsorption on both hydrogels and SiO₂-doped nanocomposite hydrogel. Considering their excellent adsorption properties, these functional hydrogels have the potential to be used as high efficiency adsorbents for removal of MB dye from contaminated water.

SUPPLEMENTARY MATERIAL

Additional data are available electronically at the pages of journal website: <http://www.shd.org.rs/JSCS/>, or from the corresponding author on request.

Acknowledgement. The authors thank the Bilecik Seyh Edebali University Central Research Laboratory for the characterization measurements. This work was supported by the Bilecik Seyh Edebali University Research Foundation (Project No.: 2017-01.BSEU.28-01).

ИЗВОД

СИНТЕЗА, КАРАКТЕРИЗАЦИЈА И АПСОРПЦИОНА ИСПИТИВАЊА
НАНОКОМПОЗИТНИХ ХИДРОГЕЛОВА И УТИЦАЈ SiO_2 НА СПОСОБНОСТ
УКЛАЊАЊА МЕТИЛЕНСКО ПЛАВОГ

SINAN TEMEL¹, ELIF YAMAN¹, NURGUL OZBAY² и FATMA OZGE GOKMEN¹

¹Central Research Laboratory, Bilecik Seyh Edebali University, 11230, Bilecik, Turkey и ²Chemical Engineering Department, Bilecik Seyh Edebali University, 11230, Bilecik, Turkey

Наноконтропозитни хидрогелови су добијени полимеризацијом преко слободних радикала акрилне киселине и *N*-винил-пиролидона у присуству SiO_2 честица. Хемијска и морфолошка структура хидрогелова је одређивана коришћењем инфрацрвене спектроскопије са Фуријеовим трансформацијама (FT-IR) и скенирајуће електронске микроскопије (FESEM). Наноконтропозитни хидрогелови су коришћени за апсорпцију и десорпцију метиленско плавог из отпадних вода. Као отпадна вода је коришћен у лабораторијским условима припремљен раствор метиленско плавог у дестилованој води. Садржај угљеника, водоника и азота у боји, хидрогеловима, као и у хидрогеловима са апсорбованом бојом, је одређен на основу елементарне анализе. Изучаван је утицај садржаја наночестица SiO_2 и састава кополимера на апсорпциони капацитет хидрогелова. Максимално уклањање боје од 98,3 % остварено са кополимерним хидрогелом AA-co-VP (3:1). Показано је да се синтетисани хидрогелови могу ефикасно користити као адсорбенси у третману отпадних вода.

(Примљено 17. маја, ревидирано 12. октобра, прихваћено 24. октобра 2019)

REFERENCES

1. J. Gomez-Pastora, E. Bringas, I. Ortiz, *Chem. Eng. J.* **256** (2014) 187 (<http://dx.doi.org/10.1016/j.cej.2014.06.119>)
2. R. Liu, X. Shen, X. Yang, Q. Wang, F. Yang, *J. Nanopart. Res.* **15** (2013) 1 (<https://doi.org/10.1007/s11051-013-1679-10>)
3. F. Ge, H. Ye, M. M. Li, B. X. Zhao, *Chem. Eng. J.* **17** (2012) 198 (<https://doi.org/10.1016/j.cej.2012.05.074>)
4. A. Debrassi, A. F. Correa, T. Vaccarin, N. Nedelko, A. Slawska-Waniewska, K. Sobczak, P. Dluzewski, J. M. Greneche, C. A. Rodrigues, *Chem. Eng. J.* **183** (2013) 284 (<https://doi.org/10.1016/j.cej.2011.12.078>)
5. A. Anglada, M. J. Rivero, I. Ortiz, A. Urriaga, *J. Chem. Technol. Biotechnol.* **83** (2008) 1339 (<https://doi.org/10.1002/jctb.1981>)
6. M. Faraji, Y. Yamini, E. Tahmasebi, A. Saleh, F. Nourmohammadian, *J. Iran. Chem. Soc.* **7** (2010) 130 (<https://doi.org/10.1007/BF03246192>)
7. A. Afkhami, R. Moosavi, *J. Hazard. Mater.* **174** (2010) 398 (<https://doi.org/10.1016/j.jhazmat.2009.09.066>)
8. F. Keyhanian, S. Shariati, M. Faraji, M. Hesabi, *Arab. J. Chem.* **9** (2011) 348 (<http://dx.doi.org/10.1016/j.arabjc.2011.04.012>)

9. B. Tasdelen, D. Izlen, S. Meric, *Colloids Surfaces, A* **519** (2017) 245 (<https://doi.org/10.1016/j.colsurfa.2016.11.003>)
10. B. H. Hameed, A. T. M. Din, A. L. Ahmad, *J. Hazard. Mater.* **141** (2007) 819 (<https://doi.org/10.1016/j.jhazmat.2006.07.049>)
11. F. Fu, Q. Wang, *J. Environ. Manage.* **92** (2011) 407 (<https://doi.org/10.1016/j.jenvman.2010.11.011>)
12. I. Fernandez-Olmo, A. Ortiz, A. Urriaga, I. Ortiz, *J. Chem. Technol. Biotechnol.* **83** (2008) 1616 (<https://doi.org/10.1002/jctb.1997>)
13. A. Urriaga, E. Bringas, R. Mediavilla, I. Ortiz, *J. Membr. Sci.* **356** (2010) 88 (<https://doi.org/10.1016/j.memsci.2010.03.034>)
14. M. F. San Roman, I. Ortiz Gandara, R. Ibanaz, I. Ortiz, *J. Membr. Sci.* **415** (2012) 616 (<https://doi.org/10.1016/j.memsci.2012.05.063>)
15. J. Saiz, E. Bringas, I. Ortiz, *J. Chem. Technol. Biotech.* **89** (2014) 909 (<https://doi.org/10.1002/jctb.4331>)
16. S. Thakur, O. Arotiba, *Ads. Sci. Technol.* **36** (2017) 458 (<https://doi.org/10.1177/0263617417700636>)
17. A. R. Hernandez-Martínez, J. A. Lujan-Montelongo, C. Silva-Cuevas, J. D. Mota-Morales, M. Cortez-Valadez, Á. J. Ruiz-Baltazar, M. Cruze, J. Herrera-Ordóñez, *React. Funct. Polym.* **122** (2018) 75 (<https://doi.org/10.1016/j.reactfunctpolym.2017.11.008>)
18. H. Dai, Y. Zhang, L. Ma, H. Zhang, H. Huang, *J. Carb. Pol.* **215** (2019) 366 (<https://doi.org/10.1016/j.carbpol.2019.03.090>)
19. F. Bergaya, C. Detellier, J. F. Lambert, G. Lagaly, *Handbook of Clay Science, Developments of Clay Science*, Elsevier, London, 2013 (eBook ISBN: 9780080457635 Hardcover ISBN:9780080441832)
20. T. Jiao, H. Zhao, J. Zhou, Q. Zhang, X. Luo, J. Hu, Q. Peng, X. Yan, *ACS Sustain. Chem. Eng.* **3** (2015) 3130 (<https://doi.org/10.1021/acssuschemeng.5b00695>)
21. T. Jiao, H. Guo, Q. Zhang, Q. Peng, Y. Tang, X. Yan, B. Li, *Sci. Rep.* **5** (2016) 11873 (<https://doi.org/10.1038/srep11873>)
22. Y. Liu, Y. Zheng, A. Wang, *Ads. Sci. Tech.* **28** (2010) 913 (<https://doi.org/10.1260/0263-6174.28.10.913>)
23. S. Thakur, S. Pandey, O. A. Arotiba, *Carbohydr. Polym.* **153** (2016) 34 (<https://doi.org/10.1016/j.carbpol.2016.06.104>)
24. K. Haraguchi, T. Takehisa, S. Fan, *Macromolecules* **25** (2002) 10162 (<https://doi.org/10.1021/ma021301r>)
25. F. Ö. Gökmen, N. Pekel-Bayramgil, *Eur. Chem. Bull.* **6** (2017) 514 (<https://doi.org/10.17628/ecb.2017.6.514-518>)
26. N. A. Peppas, A. R. Khare, *Adv. Drug Del. Rev.* **11** (1993) 1 ([https://doi.org/10.1016/0169-409X\(93\)90025-Y](https://doi.org/10.1016/0169-409X(93)90025-Y))
27. A. Singh, P. K. Sharma, V. K. Garg, G. Garg, *Int. J. Pharm. Sci. Rev. Res.* **4** (2010) 97
28. X. Sun, G. Zhang, Q. Shi, B. Tang, Z. J. Wu, *Appl. Polym. Sci.* **86** (2002) 3212 ([https://doi.org/10.1002/1097-4628\(20010404\)80:1<115::AID-APP1079>3.0.CO;2-K](https://doi.org/10.1002/1097-4628(20010404)80:1<115::AID-APP1079>3.0.CO;2-K))
29. N. Kashyap, N. Kumar, M. Kumar, *Crit. Rev. Ther. Drug* **22** (2005) 107 (<https://doi.org/10.1615/CritRevTherDrugCarrierSyst.v22.i2.10>)
30. O. V. Ovchinnikov, A. V. Evtukhova, T. S. Kondratenko, M. S. Smirnov, V. Y. Khokhlov, O. V. Erina, *Vib. Spectrosc.* **86** (2016) 181 (<https://doi.org/10.1016/j.vibspec.2016.06.016>).